Hindawi
Journal of Chemistry
Volume 2020, Article ID 5496712, 13 pages
https://doi.org/10.1155/2020/5496712

Research Article

Adsorption of Cu (II) and Cd (II) from Wastewater by Sodium Alginate Modified Materials

Yingying Zhao, Linchuan Zhan, Zhongjun Xue, Kianpoor Kalkhajeh Yusef, Hongxiang Hu, and Mengjun Wu

School of Resources and Environment, Anhui Agricultural University, Hefei 230036, China

Correspondence should be addressed to Hongxiang Hu; hongxianghu@163.com

Received 14 April 2020; Accepted 17 June 2020; Published 3 August 2020

Academic Editor: Khaled Mostafa

Natural macromolecule adsorbing materials are alternatives for remediation of heavy metals' polluted waters. In this study, sodium alginate composite gel (SACL) was synthesized from sodium alginate (SA), polyethylene glycol oxide (PEO), and nanomaterials to remove wastewater Cu (II) and Cd (II). The adsorption efficiency of SACL was analysed in relation to the contact time, initial concentrations of metal ions, temperature, adsorbent dosage, and solution pH. Three models, i.e., kinetic model, isothermal adsorption model, and thermodynamic model, were used to fit the experimental data. Our results showed that the highest removal rates of Cu (II) and Cd (II) from wastewater were 96.8% and 78%, respectively, under the condition of the best liquid-solid ratio of 12.5 ml·g^{-1}, and the contact time of 180 min (25°C). Overall, the SACL adsorption of Cu (II) and Cd (II) was spontaneous. The adsorption kinetics and the isothermal adsorption were fitted well with the pseudo-second-order kinetic equation and Langmuir equation, respectively. Combined with SEM-EDS and FTIR analysis, results suggested that SACL adsorbs wastewater Cu (II) and Cd (II) mainly through chemical reaction on its surface area. Altogether, this work concludes on SACL as an efficient and ecofriendly adsorbent for wastewater Cu (II) and Cd (II).

1. Introduction

Worldwide, the discharge of heavy metals to water bodies is still of particular concern due to electroplating, mining, smelting, and chemical industry, as well as several other industrial and agricultural activities. Water pollution of heavy metals not only harms aquatic animals and plants but also threatens human health if it enters the food chain [1]. For instance, excessive amounts of copper (Cu), the second pollutant in industrial wastewaters, can poison the chlorophyll of aquatic plants [2–4]. Furthermore, industrial wastewater is the primary pathway discharging cadmium (Cd) into the environment. An environmental threshold concentration of 0.1 mg·L^{-1} has been suggested for sewage Cd (Integrated Wastewater Discharge Standard, China). So far, several approaches such as coagulation and precipitation [5, 6], ion exchange [7], and biological treatment [8] have been practiced for the remediation of heavy metals' polluted waters. However, coagulation and precipitation and ion exchange methods are time-consuming and expensive, and they might produce secondary pollutants [9]. In contrast, biosorption methods are time-saving with high efficiency and simple operation [10]. As such, satisfactory results were seen for biochar, apatite, hydrotalcite, and manganese dioxide [11]. Alternatively, natural macromolecule adsorbing materials can also be taken into account to remove heavy metals from water samples [12]. For instance, Hamouz and Ali successfully applied polyphosphate to adsorb Pb (II) and Cu (II) from aqueous solution [13]. In another study, crab shells had a good inhibitory effect on Pb (II), Cd (II), and Cr (III) in wastewater [14]. Besides, struvite-natural zeolite composite had an excellent adsorption performance for wastewater Pb (II) with a maximum adsorption capacity of 750 mg·g^{-1} [15]. Sodium alginate (SA) is a natural polymer polysaccharide with a molecular formula of $(C_5H_7O_4COONa)n$. Environmentally, SA is nontoxic with high biodegradability. Therefore, it can be widely used as a gel matrix, membrane material, and water-blocking agent [16]. Due to its high quantities of carbonyl groups and oxygen atoms, SA is an efficient adsorbent for metal ions

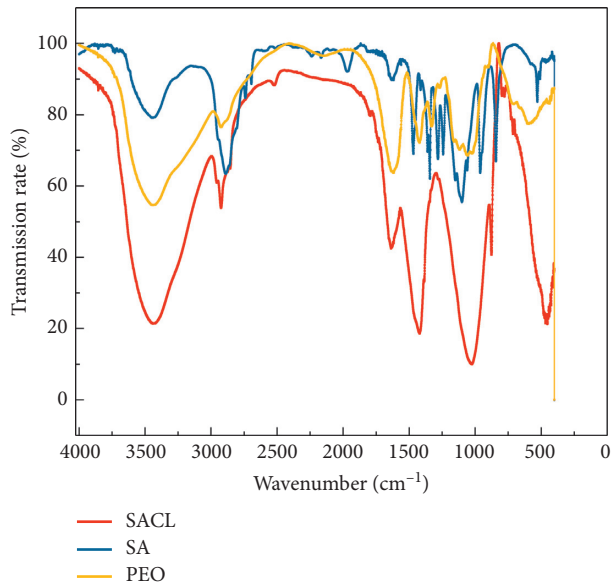

Figure 1: FTIR spectra of SACL, SA, and PEO.

[17]. However, SA does not have sufficient mechanical stability that, in turn, may result in the formation of a gel with low efficiency and damage its elasticity [18]. To respond to this challenge, cross-linking agents such as polyethylene oxides (PEO) are useful [19, 20]. PEO is a crystalline thermoplastic water-soluble polymer with the molecular formula of H-(-O-CH_2-CH_2-)n-OH. Changes in PEO molecular weight determine its properties [21]. In addition to SA, nanomaterials have been also suggested to be promising to remove environmental heavy metals due to their silica and phosphorus-containing minerals, recyclability, and specific surface area as large as 180 $m^2 \cdot g^{-1}$. Xue et al. found that mesoporous ceramic functional nanomaterials could efficiently remove wastewater Cd (II) with an adsorption rate of 97.1 $mg \cdot g^{-1}$ [22]. The hydrogel made by thermal cross-linking of polyacrylic acid and SA had significant adsorption properties for Cu (II) in water [23]. Similarly, a hydrogel made of chitosan, sodium alginate, and Ca (II) was effective to adsorb Cu (II), Cd (II), and Pb (II) in water [24]. In this study, a new type of adsorbent, sodium alginate composite gel (SACL), was prepared by synthesizing the natural polymer substance SA, the cross-linking agent PEO, and nanomaterials to remove wastewater Cu (II) and Cd (II). Hence, the results of the present work can provide a basis for wastewater treatment using green and rapidly degradable natural adsorbing materials.

2. Materials and Methods

2.1. Materials. We purchased SA and PEO from Bomei Biotechnology Co., Ltd., Hefei, China, and nanomaterials from Gefeng Co., Ltd., Wuhu, China. The stock solutions of Cu (II) and Cd (II) were prepared using $Cu(NO_3)_2 \cdot 3H_2O$ (Beilian Co., Ltd., Tianjin, China) and $CdCl_2$ (Aladdin, Shanghai, China), respectively. HCl 36%, Ca $(NO_3)_2 \cdot 4H_2O$ 99%, HNO_3 65%, $NH_3 \cdot H_2O$ 25%, and acetone 99.5% were all used as received. Deionized water was used to prepare all solutions.

2.2. Synthesis of Composite Materials. Sodium alginate composite gel (SACL) was synthesized via the method suggested by Wang et al. [25]. In accordance, SA, PEO, and nanomaterials were mixed uniformly (2 : 1 : 4). Then, 200 ml of deionized water was added to the mixture and stirred thoroughly. Afterward, the mixture was added to 0.3 $mol \cdot L^{-1}$ $Ca(NO_3)_2 \bullet 3H_2O$ solution to synthesize SACL block. The final mixture was left overnight to stabilize, and the acetone solution was continuously added to the mixture to complete the solvent exchange. All steps of SACL preparation were carried out at room temperature (25°C).

2.3. Adsorption Experiment. We investigated the capability of SACL for removal of wastewater Cu (II) and Cd (II) in relation to the contact time (30 to 300 min), initial ion concentration (50 to 1000 $mg \cdot L^{-1}$), the dosage of adsorbent (1 to 10 g), pH (1 to 5), and temperature (20 to 45°C). Batch experiments were carried out in 250 mL conical flasks containing 50 mL of Cu (II) and Cd (II) solution. To do so, all solutions were centrifuged at 3000 rpm for 20 minutes, and then the supernatant was filtered (0.45 μm membrane filter) and diluted (1 : 50) to measure the concentration of the remaining Cu (II) and Cd (II) after SACL adsorption via inductively coupled plasma emission spectrometer (ICP-AES, Thermo Scientific, Model 6000, USA). All experiments and measurements were replicated three times.

The adsorption capacity of Cu (II) and Cd (II) at equilibrium was calculated using the following equation:

$$q_e = \frac{(C - C_e) \times V}{m_0}, \quad (1)$$

where q_e is the adsorption capacity of wastewater Cu (II) and Cd (II) by SACL ($mg \cdot g^{-1}$); C and C_e are the initial and equilibrium concentrations of Cu (II) and Cd (II) in wastewater, respectively ($mg \cdot L^{-1}$); V is the solution volume (L); m_0 is the amount of added adsorbent (g).

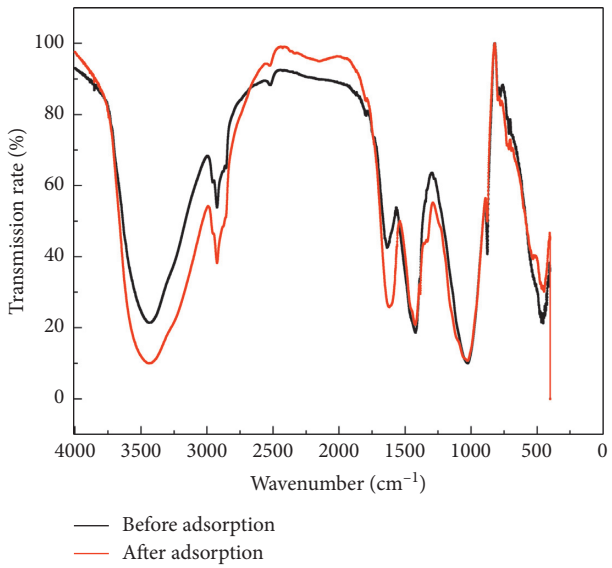

Figure 2: FTIR spectra of SACL before and after adsorption of wastewater Cu (II) and Cd (II).

Table 1: Position of the main peaks in FTIR spectra of PEO, SA, and SACL.

Wavenumber before SACL adsorption (cm^{-1})	Wavenumber after SACL adsorption (cm^{-1})	Assignment
3439	3440	-OH stretching vibration
2924	2924	-CH stretching vibration
1636	1617	C=O stretching vibration
1420	1420	C-H bending vibration
1024	1026	C-O stretching vibration
876	876	C-H bending vibration

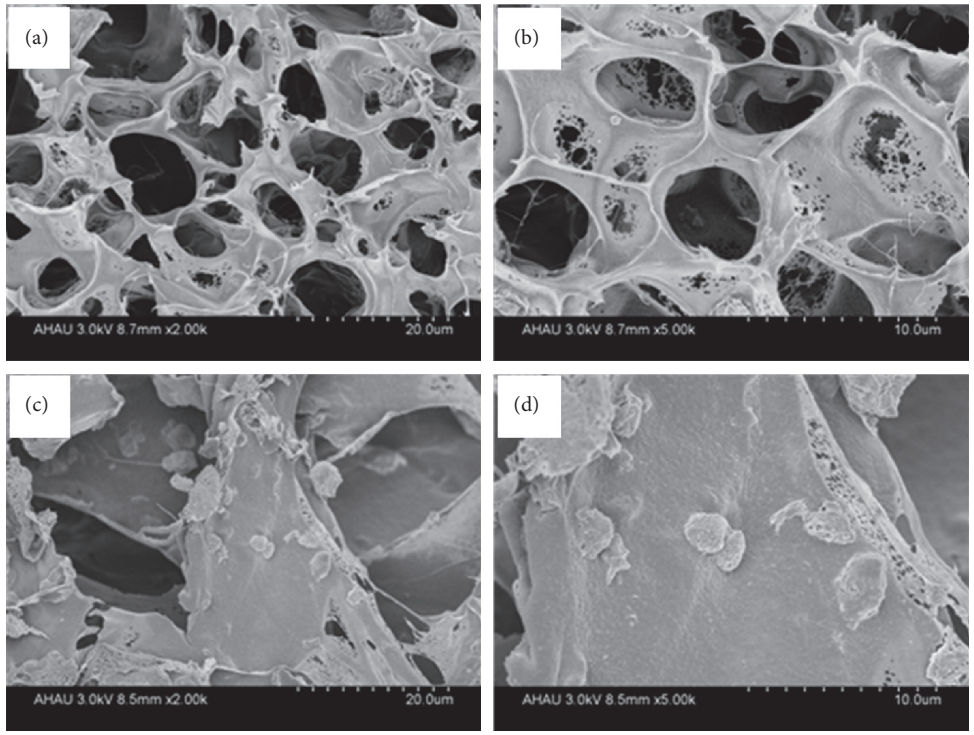

Figure 3: SEM images of SACL (a, b) before and (c, d) after adsorption of wastewater Cu (II) and Cd (II).

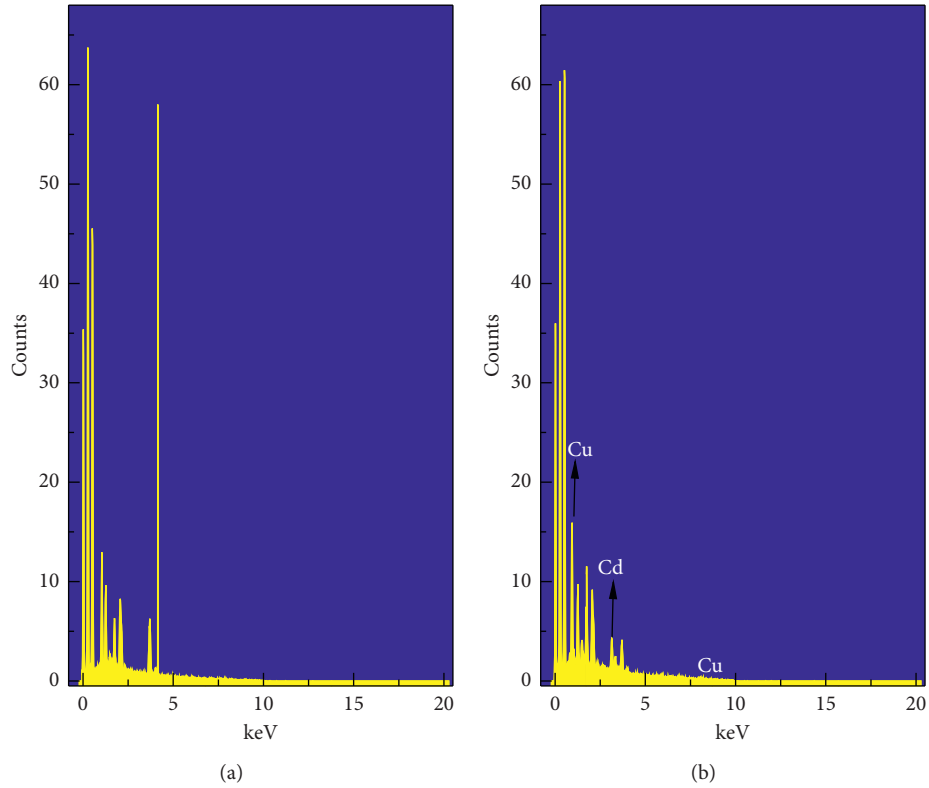

Figure 4: EDS spectra of SACL (a) before and (b) after adsorption of wastewater Cu (II) and Cd (II).

The removal rate of wastewater Cu (II) and Cd (II) by SACL was calculated using the following equation:

$$U = \frac{(C - C_e)}{C} \times 100\%, \quad (2)$$

where U is the removal rate of wastewater Cu (II) and Cd (II) by SACL (%); C and C_e are the initial and equilibrium concentrations of Cu (II) and Cd (II) in wastewater, respectively ($mg \cdot L^{-1}$).

2.4. Characterization Techniques. Morphology, structure, and dispersion of SACL before and after adsorption were characterized by a scanning electron microscope (SEM, S-4800, Hitachi, Japan), and the functional groups of SACL before and after adsorption were obtained using Fourier transform infrared spectroscopy (FTIR). The FTIR spectra were recorded between 4000 and 400 cm^{-1} using a Nicolette iS50 (Thermo Scientific, USA) spectrometer.

Table 2: Elemental mass ratio before and after SACL adsorption in EDS spectrum.

Element	Mass ratio (%)
Before adsorption	
C	47.6
O	37.6
Si	1.6
Ca	6.4
Na	4.0
Cu	—
Cd	—
After adsorption	
C	38.9
O	37.2
Si	2.7
Ca	2.6
Na	—
Cu	9.7
Cd	6.1

3. Results and Discussion

3.1. Characterization of SACL. The FTIR spectra and peaks of SACL, SA, and PEO are shown in Figure 1, respectively. Accordingly, changes occurred in almost all the peak values of the synthesized SACL, indicating successful combination of SA and PEO. Furthermore, changes took place in the peak values of SACL after adsorption of wastewater Cu (II) and Cd (II) (Figure 2; Table 1). A broadened -OH stretching vibration adsorption peak appeared at 3440 cm^{-1}, mainly caused by -OH ion of SACL; -CH stretching vibration peak appeared at 2924 cm^{-1}; C=O stretching vibration peaks appeared at 1617 cm^{-1} ; C-H bending vibration peak appeared at 1420 cm^{-1}; C-O stretching vibration peak appeared at 1026 cm^{-1}; C-H bending vibration absorption occurred at 876 cm^{-1}. The change of the peak value of SACL indicates that SACL can effectively adsorb Cu (II) and Cd (II) in the waste water, thereby causing the peak value to move or weaken.

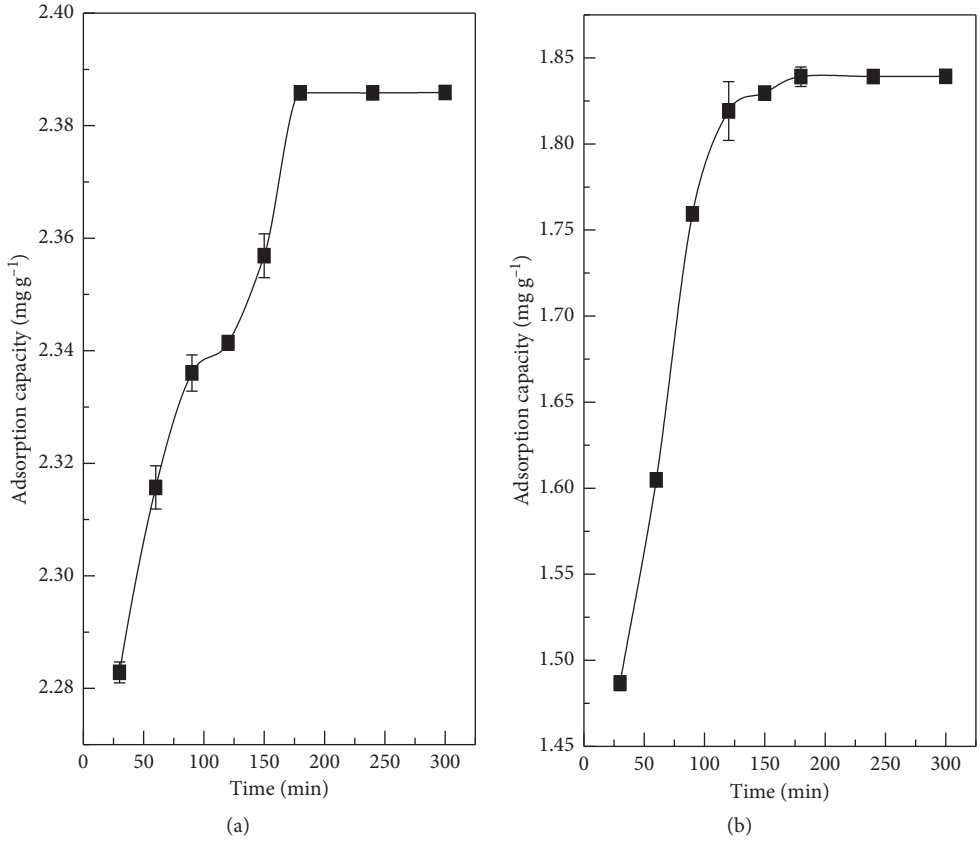

Figure 5: The effect of contact time on adsorption of wastewater (a) Cu (II) and (b) Cd (II) by SACL (experimental condition: Cu (II) concentration = 200 mg·L^{-1}; Cd (II) concentration = 200 mg·L^{-1}; amount of adsorbent = 4 g; pH = 4; temperature = 25°C; and agitation speed = 150 rpm) (error bars represent the standard deviation of three replicates).

Before adsorption experiment, SACL had numerous pores of different shapes and specifications (Figures 3(a) and 3(b)), facilitating Cu (II) and Cd (II) transmission into its inner structure [1]. After adsorption, multiple small particles appeared on the inner surface of SACL (Figures 3(c) and 3(d)). These observations and analyses revealed that SACL removes metal ions not only through pore filling but also through adsorption on its inner surface.

From Figure 4, large absorption peaks appeared for C and O before and after SACL adsorption of wastewater Cu (II) and Cd (II). This is due to the high contents of C and O elements in SACL. The adsorption peaks of Cu (II) and Cd (II) by SACL were 9.7% and 6.1%, respectively, suggesting that SACL has certain adsorption capacities for these metal ions (Table 2).

3.2. Adsorption Studies and Analysis

3.2.1. Effect of Contact Time. The effect of contact time on SACL adsorption of wastewater Cu (II) and Cd (II) is shown in Figure 5. Results indicated that, with increasing the contact time from 180 to 300 min, adsorption of Cu (II) and Cd (II) increased, but then flattened. This is consistent with the findings of Tong et al. [26]. Therefore, increasing the adsorption of metal ions might be attributed to the gradual occupation of the adsorption sites of SACL in the early stage of adsorption process, whereas occupation of the adsorption sites of SACL to almost the saturation level can be the cause of the flattened adsorption [27].

3.2.2. Effect of Initial Ion Concentration. The SACL adsorption of wastewater Cu (II) and Cd (II) in relation to their initial solution concentrations is shown in Figure 6. In accordance, increases in the solution concentration of Cu (II) and Cd (II) increased their adsorption capacity by SACL. Nonetheless, the removal rates of wastewater Cu (II) and Cd (II) increased at first but then decreased. Hence, the removal rates of Cu (II) and Cd (II) reached their maximum values of 95.6% and 71.3%, respectively, at their solution concentration of 200 mg·L^{-1}. This is in agreement with the results of Nag et al. [28]. At low solution concentration of metal ions, the number of effective collisions increased between SACL and metal ions, which may have led to the occupation of the effective sites on the adsorbent. This, therefore, increased the adsorption capacity. High solution concentration of metal ions may have led to the occupation of the effective adsorption sites on the surface of SACL, thereby reaching the

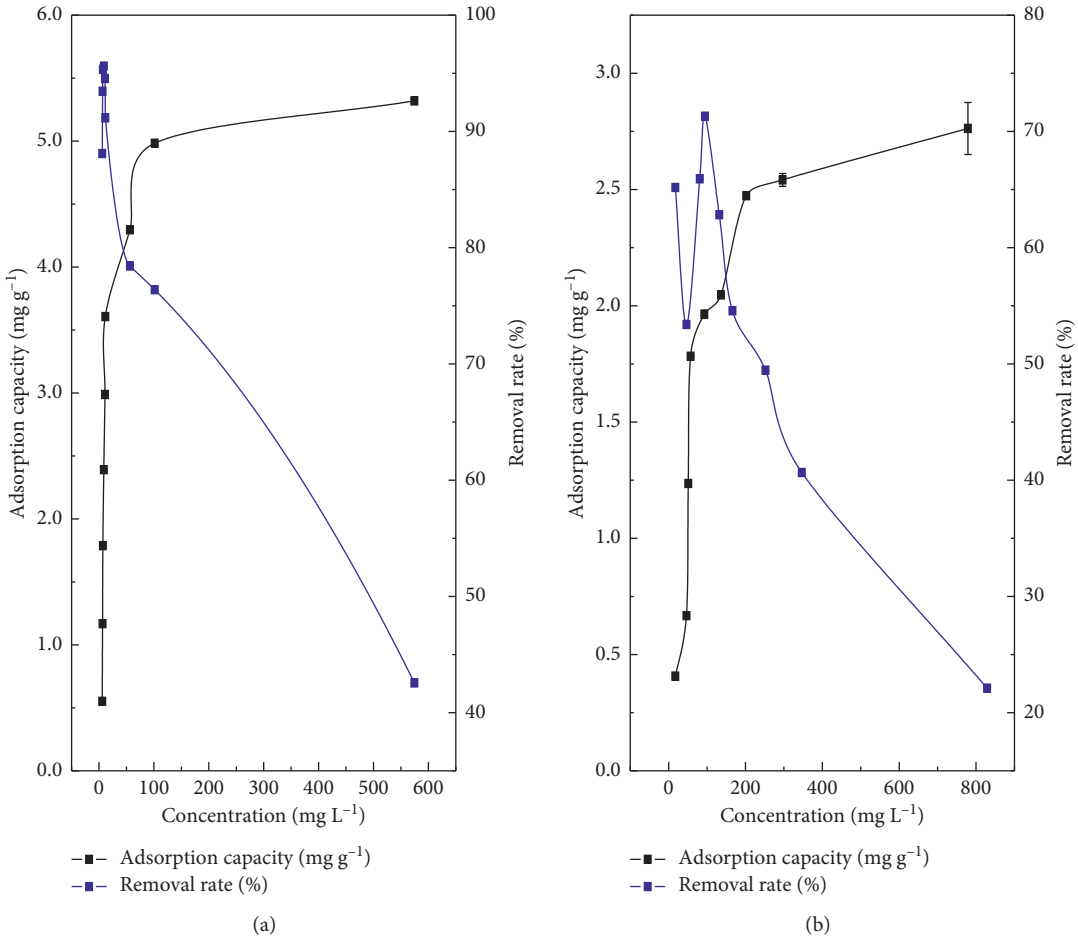

Figure 6: Effect of initial ion concentration on the adsorption of wastewater (a) Cu (II) and (b) Cd (II) by SACL (experimental condition: contact time = 180 min; amount of adsorbent = 4 g; pH = 4; temperature = 25°C; and agitation speed = 150 rpm) (error bars represent the standard deviation of three replicates).

saturation level. This stabilized the adsorption rates of Cu (II) and Cd (II) by SACL [29].

3.2.3. Effect of Adsorbent Dosage. The removal rates of Cu (II) and Cd (II) in relation to the dosage of SACL are shown in Figure 7. Overall, an increase in SACL dosage increased the removal of solution metal ions. At SACL dosage of 80 mg·L^{-1}, the removal rates of Cu (II) and Cd (II) reached their maximum. Then after, increasing SACL dosage did not affect adsorption of Cu (II) and Cd (II). This might be attributed to the low mass of added SACL, which has led to the rapid occupation of the adsorption sites on the surface of SACL. Correspondingly, increasing the amount of SACL increased the adsorption sites. Nevertheless, increasing the dosage of SACL to over 80 mg·L^{-1} may have increased its agglomeration. The latter might cause overlap of adsorbents that, in turn, limits the specific surface area of the adsorbents and consequently affects the adsorption results [30].

3.2.4. Effect of pH. Figure 8 shows the effect of solution pH on the removal rates of wastewater Cu (II) and Cd (II). As shown in Figure 8, high solution pH might have hydrolyzed the metal ions. This can cause hydroxide precipitation of solution Cu (II) and Cd (II), affecting their adsorption by SACL [31]. Hence, pH values higher than 5 were not set in this experiment. Overall, the amount of SACL adsorption of Cu (II) increased with increasing solution pH (Figure 8(a)). At solution pH above 4, a slight increase appeared in the amount of Cu (II) adsorption, and then it gradually turned into constant. In contrast, at solution pH of 4, the amount of SACL adsorption of Cd (II) reached its maximum (1.83 mg·g^{-1}) (Figure 8(b)). Afterward, Cd (II) adsorption shifted downward with increasing solution pH. The negligible adsorption capacities of Cu (II) and Cd (II) at low solution pH are attributed to the presence of high quantities of H^+. Therefore, the surface of the adsorbent repels Cu (II) and Cd (II), increasing their migration resistance and decreasing their adsorption [32, 33]. Solution pH of above 6 increases the concentration of OH^-, gradually decreasing the repulsion resistance of Cu (II) and Cd (II) and their adsorption by SACL [34]. Furthermore, at pH > 6, solution OH^- forms hydrated hydroxyl complex with Cu (II) and Cd (II), reducing their adsorption by SACL [35].

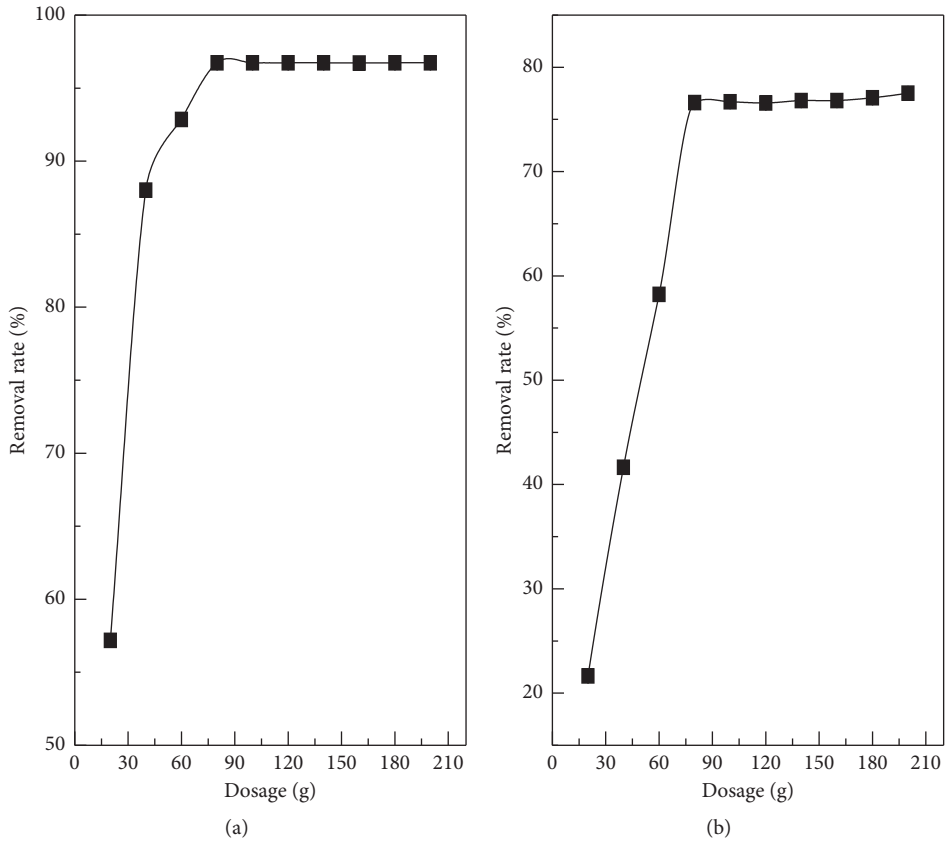

Figure 7: Effect of adsorbent dosage on the adsorption of wastewater (a) Cu (II) and (b) Cd (II) by SACL (experimental condition: Cu (II) concentration = 200 mg·L^{-1}; Cd (II) concentration = 200 mg·L^{-1}; contact time = 180 min; pH = 4; temperature = 25°C; and agitation speed = 150 rpm) (error bars represent the standard deviation of three replicates).

3.2.5. Effect of Temperature. Figure 9 illustrates the removal rates of Cu (II) and Cd (II) in relation to temperature. As can be seen, an increase in temperature gradually increased the adsorption of wastewater Cu (II) and Cd (II) by SACL, suggesting that SACL adsorption of these metal ions is an endothermic process. This is consistent with the findings of Chowdhury and Saha and Hu et al. [36, 37]. This might be justified by enlarging the molecular diffusion inside Cu (II) and Cd (II) due to the increasing temperature, facilitating their adsorption by SACL [38]. Nevertheless, high temperatures can decrease the viscosity of SACL. Hence, we did not set temperatures higher than 45°C.

3.3. Adsorption Mechanism

3.3.1. Adsorption Kinetics. The adsorption rate of metal ions is determined by their migration from the solution to adsorbing sites. This is a time dependent process. To explore the adsorption process of metal ions by SACL in relation to time, the adsorption models were employed. Therefore, the experimental data were fitted with the pseudo-first-order kinetic model (in (3)) and the pseudo-second-order kinetic model (in (4)) as follows [39, 40]:

$$q_a = B - B \quad \exp^{(-Bt)}, \tag{3}$$

$$\frac{1}{q_a} = B + \frac{A}{t}, \tag{4}$$

where q_a is the amount of adsorption for a period of time (mg·g^{-1}); t is time (min); A and B are the model parameters.

Data of SACL adsorption of wastewater Cu (II) and Cd (II) at different times fitted with the adsorption kinetic models are presented in Table 3. Based on the determination coefficients (R^2) and standard errors, our results revealed that the pseudo-second-order dynamic model was superior, suggesting that it explains better the SACL adsorption of wastewater Cu (II) and Cd (II). Besides, the pseudo-second-order kinetic model is used to prove that the chemical reaction rate is related to the restrictive steps [41]. This suggests that Cu (II) and Cd (II) adsorption by SACL is a chemical process, and the adsorption sites determine the adsorption rate.

3.3.2. Adsorption Isotherm. The isothermal adsorption of Cu (II) and Cd (II) by SACL is fitted with Langmuir and Freundlich models via (5) and (6), respectively [42]:

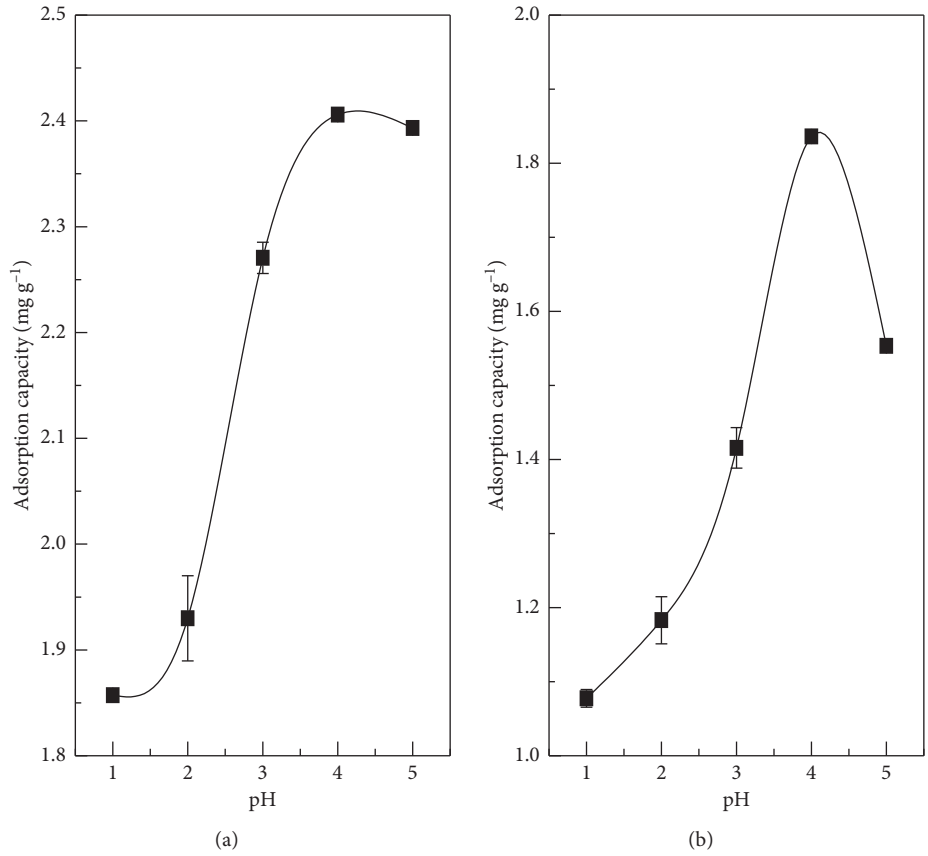

Figure 8: Effect of solution pH on the adsorption of wastewater (a) Cu (II) and (b) Cd (II) by SACL (experimental condition: Cu (II) concentration = 200 mg·L^{-1}; Cd (II) concentration = 200 mg·L^{-1}; contact time = 180 min; amount of adsorbent = 4 g; temperature (25°C); and agitation speed = 150 rpm) (error bars represent the standard deviation of three replicates).

$$q = q_n \frac{k_l p_e}{1 + k_l p_e}, \tag{5}$$

$$q = k_s p_e \left(\frac{1}{n}\right), \tag{6}$$

where q is the equilibrium adsorption quantity (mg·g^{-1}); q_n is the maximum amount of adsorption (mg·g^{-1}); p_e is the equilibrium concentration (mg·L^{-1}); n, k_l, and k_e are the adsorption constants.

Langmuir adsorption isotherm equation can also define a dimensionless separation factor (Rl) using the following expression:

$$Rl = \frac{1}{1 + k_l C}. \tag{7}$$

Rl can be used to indicate the nature of the adsorption process. Accordingly, the adsorption is unfavourable if $Rl > 1$, the adsorption behaviour is linear if $Rl = 1$, and the adsorption is irreversible if $Rl = 0$ [43].

From Table 4, it was demonstrated that the determination coefficients of Langmuir model were higher than those of Freundlich model. In addition, the maximum adsorption amount obtained by fitting Langmuir model was close to the actual adsorption amount; hence, it can better describe the behaviour of SACL adsorption of Cu (II) and Cd (II). Since Langmuir isotherm equation is a single-molecule adsorption equation [44, 45], we can conclude that the adsorption of Cu (II) and Cd (II) occurred on SACL surface. However, the Rl values were $0 < Rl < 1$, indicating that the adsorption of Cu (II) and Cd (II) by SACL is favourable.

3.3.3. Adsorption Thermodynamics. The present study examined the SACL adsorption process of Cu (II) and Cd (II) ions in relation to temperature via Gibbs free energy change (ΔG), enthalpy change (ΔH), and entropy change (ΔS) as expressed by the following equations:

$$k = -\frac{C_a}{C_i}, \tag{8}$$

$$\ln k = -\frac{\Delta H}{RT} + \frac{\Delta S}{R}, \tag{9}$$

$$\Delta G = -RTLnk, \tag{10}$$

where k is the constant; C_a is the equilibrium concentrations of Cu (II) and Cd (II) (mg·L^{-1}); C_i is the residual concentrations of Cu (II) and Cd (II) (mg·L^{-1}); R is the ideal gas

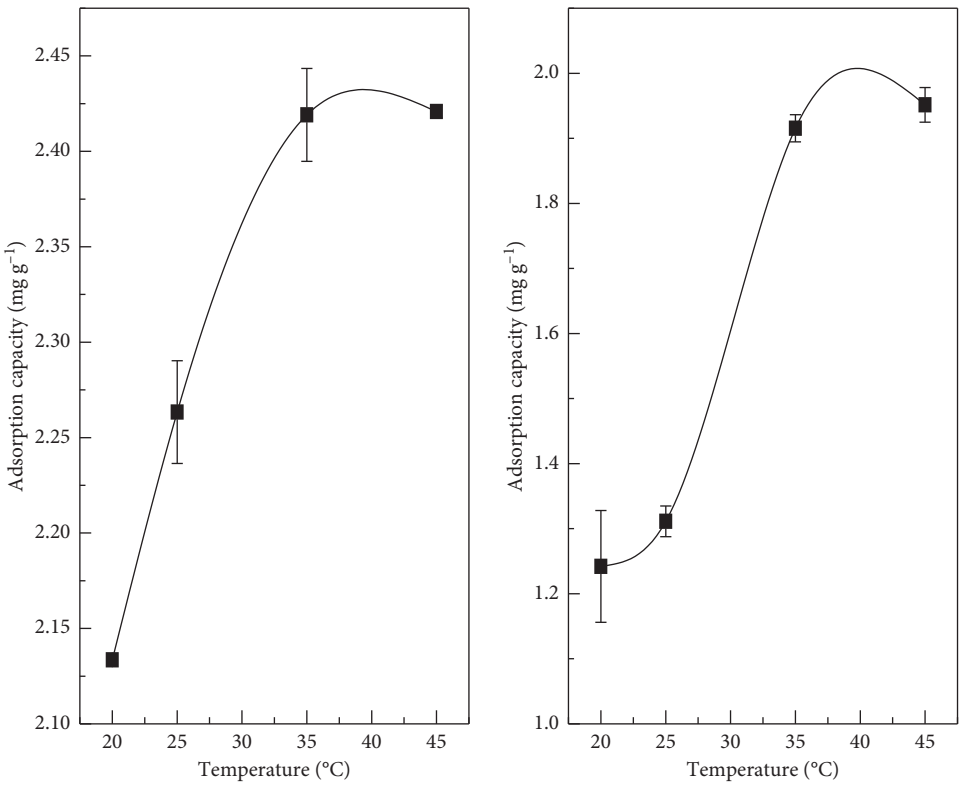

Figure 9: Effect of temperature on the adsorption of wastewater (a) Cu (II) and (b) Cd (II) by SACL (experimental condition: Cu (II) concentration = 200 mg·L^{-1}; Cd (II) concentration = 200 mg·$^{-1}$; contact time = 180 min; amount of adsorbent = 4 g; pH = 4; and agitation speed = 150 rpm) (error bars represent the standard deviation of three replicates).

Table 3: Fitting parameters of two kinetic models for Cu (II) and Cd (II) adsorption by SACL.

	Pseudo-first-order kinetic model				Pseudo-second-order kinetic model			
	A	B	R^2	ε^2	A	B	R^2	ε^2
Cu (II)	0.003	2.451	0.848	0.029	2.406	0.176	0.999	0.001
Cd (II)	0.002	1.411	0.612	0.002	0.249	30.590	0.999	0.007

Table 4: Isothermal parameters of adsorption of Cu (II) and Cd (II) by SACL at different temperatures.

Metal ion	T (K)	Langmuir model			Fruendlich model		
		Q_n (mg·g^{-1})	K_l	R^2	K_s	$1/n$	R^2
Cu (II)	288	4.377	0.047	0.929	0.253	0.988	0.741
	298	5.608	0.062	0.917	0.458	0.761	0.674
	308	6.783	0.063	0.889	0.470	0.809	0.657
Cd (II)	288	1.39	0.013	0.943	7.070	4.146	0.862
	298	3.035	0.017	0.944	0.126	1.126	0.910
	308	3.426	0.015	0.952	0.067	1.531	0.709

constant, 8.314 (J·mol^{-1}·K^{-1}); and T is the adsorption temperature (K).

As presented in Table 5, the negative ΔG values indicate that the SACL adsorption of Cu (II) and Cd (II) is spontaneous [46], and the rate of adsorption decreased with increasing temperature. In contrast, ΔH had positive values, indicating that the SACL adsorption of Cu (II) and Cd (II) is an endothermic process. However, ΔS positive values indicate that SACL adsorption of Cu (II) and Cd (II) is a process of increasing entropy [47].

Table 5: Thermodynamic parameters of SACL adsorption of wastewater Cu (II) and Cd (II).

Metal ion	T (K)	ΔG (kJ·mol^{-1})	ΔH (kJ·mol^{-1})	ΔS (J·mol^{-1}·K^{-1})
Cu (II)	288	−677.137	7.630	2289.955
	298	−690.036		
	308	−712.936		
Cd (II)	288	−363.641	3.009	1252.197
	298	−376.163		
	308	−388.685		

Table 6: Basic properties of Cu (II) and Cd (II).

Metal ion	Hydration radius	Electronegativity
Cu (II)	0.419	1.90
Cd (II)	0.426	1.69

Table 7: Adsorption of Cu (II) and Cd (II) by SACL compared with the previously reported composite materials.

Adsorbent	Initial concentration ($mg{\cdot}L^{-1}$)	Cu (II) removal rate (%)	Cd (II) removal rate (%)	References
Mag-bentonite/carboxymethyl CTS/SA hydrogel beads	50	92.6	—	[47]
SA-TSC flocculant	1000	86.3	80	[52]
SA-based attapulgite foams	250	—	88	[53]
Cocoa skin-SA composite	100	95.3	—	[54]
Fe_3O_4 NPs-SA beads	250	—	90	[55]
Phosphate-embedded calcium SA beads	25	—	80	[56]
SACL	200	96.8	78	This work

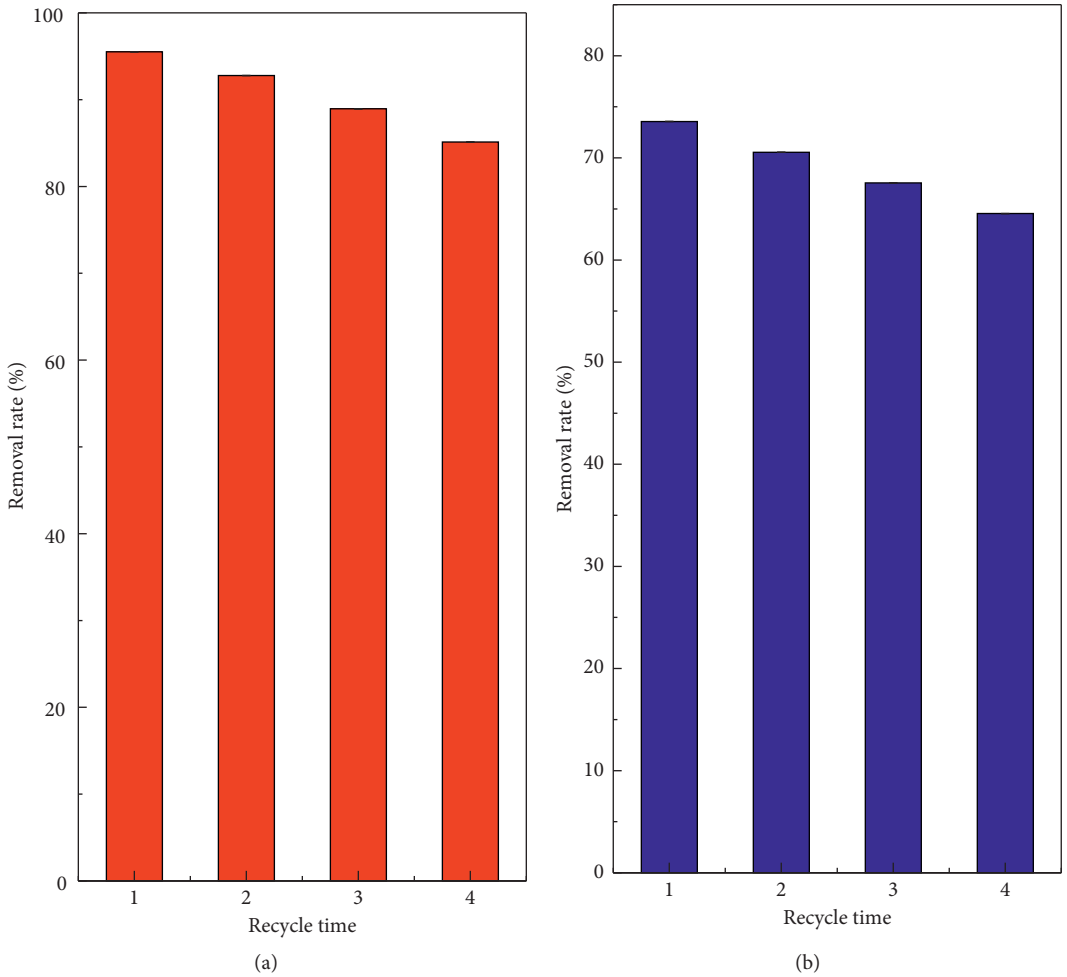

Figure 10: The removal efficiency of SACL for wastewater Cu (II) and Cd (II) after four adsorption-desorption cycles (experimental condition: Cu (II) concentration = 200 $mg{\cdot}L^{-1}$; Cd (II) concentration = 200 $mg{\cdot}L^{-1}$; contact time = 180 min; amount of adsorbent = 4 g; pH = 4; and agitation speed = 150 rpm) (error bars represent the standard deviation of three replicates).

3.3.4. Interaction Mechanism. Enormous carboxyl and hydroxyl functional groups on the SACL surface can directly adsorb metal ions. In addition, Ca (II) on the surface of SACL can be exchanged with Cu (II) and Cd (II), thereby reducing their concentration in wastewater. Nanomaterials contain a large number of cations, which will undergo ion exchange reactions with Cu (II) and Cd (II) [47]. In addition, the specific surface area of the nanomaterials is large, and Cu

(II) and Cd (II) can also be adsorbed in this way. Therefore, combining SA with nanomaterials can significantly increase the effective adsorption sites and capacity of SACL for Cu (II) and Cd (II) removal. Furthermore, the physiochemical properties of metal ions determine their adsorption [48]. Besides, in a binary system, competitive adsorption occurs between the metal ions, differentiating their adsorption amount. Herein, the SACL adsorption capacity for Cu (II) was higher than for Cd (II). This can be justified by the polarity of water molecules; hence, the negative charge of water oxygen atom can form a ligand with metal ions. In accordance, the lower SACL adsorption of Cd (II) is attributed to its larger hydration radius, resulting in a weak ligand with oxygen atoms (Table 6) [49, 50]. Conversely, the oxygen atoms of SACL easily form covalent bonds with the metal ions with strong electronegativity, resulting in a higher amount of Cu (II) adsorption (Table 6) [51].

3.4. The SACL Adsorption of Cu (II) and Cd (II) Compared with the Existing Literature. The capabilities of different adsorbing materials after modification of sodium alginate (SA), as raw material, to remove Cu (II) and/or Cd (II) are shown in Table 7. Overall, SA modification improves its adsorption performance of metal ions. As can be seen from Table 7, the previous works mainly focused on the adsorption of single ion or ions of the same period. Meanwhile, in this study, we successfully applied SACL to simultaneously adsorb Cu (II) and Cd (II) with different periods.

3.5. Reusability of SACL. To investigate the reusability of SACL, desorption experiments were carried out with 0.05 mol·L^{-1} HNO_3. As shown in Figure 10, after four desorption cycles, the removal rates of Cu (II) and Cd (II) by SACL were still as high as 85% and 60%, respectively. These values verified the strong reusability of SCAL for removal of metal ions. However, decreasing the removal rates of metal ions may be due to the weight loss of SACL after four times' desorption [57].

4. Conclusions

In this study, we successfully prepared sodium alginate composite gel (SACL) from sodium alginate (SA) to remove Cu (II) and Cd (II) from wastewater in relation to several parameters (e.g., temperature, pH, dosage of adsorbent, initial concentration of metal ions, and contact time). The maximum removal rates of Cu (II) and Cd (II) were 96.8% and 78%, respectively, under the optimum experimental condition of liquid-solid ratio of 12.5 mg·L^{-1}, rotation speed of 150 rpm, temperature of 25°C, and contact time of 180 min. The experimental data confirmed that the pseudo-second-order kinetic model could fit well the SACL adsorption of Cu (II) and Cd (II). The isothermal adsorption model revealed that Langmuir equation was superior to describe Cu (II) and Cd (II) adsorption by SACL. Thermodynamic model showed that adsorption of Cu (II) and Cd (II) by SACL was spontaneous. Nevertheless, there were still adsorption sites remaining on the SACL surface, which could sufficiently adsorb wastewater Cu (II) and Cd (II). Altogether, our results concluded on SACL as a cheap adsorbent for rapid removal of Cu (II) and Cd (II) from wastewater, which might also provide a scientific basis for removal of other heavy metals from water environments.

Data Availability

The data used to support the findings of this study are included within the article.

Conflicts of Interest

The authors declare no conflicts of interest.

Authors' Contributions

Yingying Zhao conceived the experiment and conducted experimental work, drafted the manuscript, and made a series of modifications. Linchuan Zhan helped analyse the experimental data. Zhongjun Xue proposed experimental suggestions for improvement during the experiment. Hongxiang Hu and Yusef Kianpoor Kalkhajeh made suggestions for the manuscript, which greatly helped the completion of the thesis. Mengjun Wu participated in the recording and collection of experimental data. All authors gave approval for publication.

Acknowledgments

This work was financially supported by the National Key Research and Development Program of China (2016YED0801105 and 2018YED0800203).

References

[1] J. Zhang, X. Chen, Q. Liu, and L. Wu, "Distribution and potential risk assessment of heavy metals in the main estuaries of lake Poyang tributaries," *Resources and Environment in the Yangtze Basin*, vol. 23, no. 1, pp. 93–101, 2014.

[2] A. Basile, S. Sorbo, M. Cardi et al., "Effects of heavy metals on ultrastructure and Hsp70 induction in *Lemna minor* L. exposed to water along the Sarno River, Italy," *Ecotoxicology and Environmental Safety*, vol. 114, pp. 93–101, 2015.

[3] P. M. C. Antunes, M. L. Scornaienchi, and H. D. Roshon, "Copper toxicity to *Lemna minor* modelled using humic acid as a surrogate for the plant root," *Chemosphere*, vol. 88, no. 4, pp. 389–394, 2012.

[4] S. Chowdhury and P. D. Saha, "Biosorption kinetics, thermodynamics and isosteric heat of sorption of Cu (II) onto *Tamarindus indica* seed powder," *Colloids and Surfaces B: Biointerfaces*, vol. 88, no. 2, pp. 697–705, 2011.

[5] Q. Chang, Y. An, and M. Q. Yu, "Preparation of polymer heavy metal flocculant and treatment of wastewater containing copper," *Environment Chemistry*, vol. 25, no. 2, pp. 176–179, 2006.

[6] N. Rajesh, A. S. K. Kumar, S. Kalidhasan, and V. Rajesh, "Trialkylamine impregnated macroporous polymeric sorbent for the effective removal of chromium from industrial wastewater," *Journal of Chemical & Engineering Data*, vol. 56, no. 5, pp. 2292–2304, 2011.

[7] F.-F. Ma, B.-W. Zhao, and J.-R. Diao, "Adsorptive characteristics of cadmium onto biochar produced from pyrolysis of wheat straw in aqueous solution," *China Environmental Science*, vol. 37, no. 2, pp. 551–559, 2017.

[8] C. Yan, Z. He, Z. Ge, X. Sheng, and L. He, "Comparative study on adsorption characteristics of lead and cadmium by two heavy metal resistant bacteria," *Acta Scientiae Circumstantiae*, vol. 38, no. 9, pp. 3597–3604, 2018.

[9] E. A. Deliyanni, E. N. Peleka, and K. A. Matis, "Modeling the adsorption of metal ions from aqueous solution by iron-based adsorbents," *Journal of Hazardous Materials*, vol. 172, no. 2-3, pp. 550–558, 2009.

[10] I. Mobasherpour, E. Salahi, and M. Pazouki, "Comparative of the removal of Pb^{2+}, Cd^{2+} and Ni^{2+} by nano crystallite hydroxyapatite from aqueous solutions: adsorption isotherm study," *Arabian Journal of Chemistry*, vol. 5, no. 4, pp. 439–446, 2012.

[11] Y. Wu, S. Z. Zhang, X. Y. Guo, and H. L. Huang, "Adsorption of chromium (III) on lignin," *Bioresource Technology*, vol. 5, no. 4, pp. 7709–7715, 2008.

[12] O. C. S. A. Hamouz and S. A. Ali, "Novel cross-linked polyphosphonate for the removal of Pb^{2+} and Cu^{2+} from aqueous solution," *Industrial & Engineering Chemistry Research*, vol. 51, no. 43, pp. 14178–14187, 2012.

[13] D. S. Kim, "The removal by crab shell of mixed heavy metal ions in aqueous solution," *Bioresource Technology*, vol. 87, no. 3, pp. 355–357, 2003.

[14] M. J. Deng, X. J. Wang, X. J. Cheng, H. P. Jing, and J. F. Zhao, "Removal of lead ions from water by struvite natural zeolite composite," *Environmental Science*, vol. 40, no. 3, pp. 1310–1317, 2019.

[15] H. H. Tønnesen and J. Karlsen, "Alginate in drug delivery systems," *Drug Development and Industrial Pharmacy*, vol. 28, no. 6, pp. 621–630, 2002.

[16] M. Z. I. Mollah, M. A. Khan, M. A. Hoque, and A. Aziz, "Studies of physico-mechanical properties of photo-cured sodium alginate with silane monomer," *Carbohydrate Polymers*, vol. 72, no. 2, pp. 349–355, 2008.

[17] T. E. Timell, "The acid hydrolysis of glycosides: I general conditions and the effect of the nature of the aglycone," *Canadian Journal of Chemistry*, vol. 42, no. 6, pp. 1456–1472, 2011.

[18] S. I. Jeong, M. D. Krebs, C. A. Bonino, S. A. Khan, and E. Alsberg, "Electrospun alginate nanofibers with controlled cell adhesion for tissue engineering," *Macromolecular Bioscience*, vol. 10, no. 8, pp. 934–943, 2010.

[19] S. V. G. Nista, J. Bettini, and L. H. I. Mei, "Coaxial nanofibers of chitosan–alginate–PEO polycomplex obtained by electrospinning," *Carbohydrate Polymers*, vol. 127, pp. 222–228, 2015.

[20] J. Hodge and C. Quint, "The improvement of cell infiltration in an electrospun scaffold with multiple synthetic biodegradable polymers using sacrificial PEO microparticles," *Journal of Biomedical Materials Research Part A*, vol. 107, no. 9, pp. 1954–1964, 2019.

[21] Z. J. Xue, N. Liu, H. X. Hu et al., "Adsorption of Cd (II) in water by mesoporous ceramic functional nanomaterials," *Royal Society Open Science*, vol. 6, no. 4, pp. 182195–182205, 2019.

[22] M. Wang, X. Li, T. H. Zhang et al., "Eco-friendly poly (acrylic acid)-sodium alginate nanofibrous hydrogel: a multifunctional platform for superior removal of Cu (II) and sustainable catalytic applications," *Colloids and Surfaces A: Physicochemical and Engineering Aspects*, vol. 558, pp. 228–241, 2018.

[23] S. X. Tang, J. Y. Yang, L. Z. Lin et al., "Construction of physically crosslinked chitosan/sodium alginate/calcium ion double-network hydrogel and its application to heavy metal ions removal," *Chemical Engineering Journal*, vol. 393, pp. 124728–124763, 2020.

[24] Y. B. Lin, J. Xing, W. G. Sun, and T. J. Cai, "Heavy metal removal from wastewater using a granular SA-PEO gel adsorbent," *Environmental Pollution & Control*, vol. 3, pp. 50–53, 2008.

[25] T. T. Wang, J. B. Ma, D. Qu, X. Y. Zhang, J. Y. Zheng, and X. C. Zhang, "Characteristics and mechanism of copper adsorption from aqueous solutions on biochar produced from sawdust and apple branch," *Environmental Science*, vol. 38, no. 5, pp. 2161–2171, 2017.

[26] D. S. Tong, F. Kai, H. Y. Yang, J. Wang, C. H. Zhou, and H. Wei, "Efficient removal of copper ions using a hydrogel bead triggered by the cationic hectorite clay and anionic sodium alginate," *Environmental Science and Pollution Research International*, vol. 26, no. 16, pp. 16482–16492, 2019.

[27] Z.-H. Hu, A. M. Omer, X.-K. Ouyang, and D. Yu, "Fabrication of carboxylated cellulose nanocrystal/sodium alginate hydrogel beads for adsorption of Pb (II) from aqueous solution," *International Journal of Biological Macromolecules*, vol. 108, pp. 149–157, 2018.

[28] S. Nag, A. Mondal, D. N. Roy, N. Bar, and S. K. Das, "Sustainable bioremediation of Cd (II) from aqueous solution using natural waste materials: kinetics, equilibrium, thermodynamics, toxicity studies and GA-ANN hybrid modelling," *Environmental Technology & Innovation*, vol. 11, pp. 83–104, 2018.

[29] V. K. Gupta, A. Rastogi, and A. Nayak, "Biosorption of nickel onto treated alga (oedogonium hatei): application of isotherm and kinetic models," *Journal of Colloid and Interface Science*, vol. 343, no. 2, pp. 533–539, 2010.

[30] J. Cai, W. M. Ding, and Y. M. Wang, "Adsorption of copper ion by modified sawdust," *Chinese Journal of Environmental Engineering*, vol. 12, no. 10, pp. 7109–7113, 2016.

[31] A. Roy and J. Bhattacharya, "Removal of Cu (II), Zn (II) and Pb (II) from water using microwave-assisted synthesized maghemite nanotubes," *Chemical Engineering Journal*, vol. 211-212, pp. 493–500, 2012.

[32] Y. Liu, L. S. Hu, B. Tan et al., "Adsorption behavior of heavy metal ions from aqueous solution onto composite dextran-chitosan macromolecule resin adsorbent," *International Journal of Biological Macromolecules*, vol. 141, pp. 738–746, 2019.

[33] D. Ocinski, I. Jacukowicz-Sobala, and E. Kociolek-Balawejder, "Alginate beads containing water treatment residuals for arsenic removal from water—formation and adsorption studies," *Environmental Science and Pollution Research*, vol. 23, no. 24, pp. 24527–24539, 2016.

[34] Y. Xiao, C.-J. Ge, L. Zhang, F.-Z. Li, L. Yue, and H.-M. Yu, "Adsorption performance of Cd^{2+} and Cu^{2+} in aqueous solution by biochars prepared from manioc wastes," *Journal of Agro-Environment Science*, vol. 35, no. 8, pp. 1587–1594, 2016.

[35] W.-R. Liu, Q.-W. Guo, R.-B. Yang, Z.-C. Xu, and D. Zeng, "Study on removal cadmium by coagulation method and the stability of flocs," *Journal of Soil and Water Conservation*, vol. 26, no. 6, pp. 80–84, 2012.

[36] X. L. Hu, L. Li, T. J. Gong, J. Q. Zhang, J. P. Yan, and Y. W. Xue, "Enhanced alginate-based microsphere with the pore-forming agent for efficient removal of Cu (II)," *Chemosphere*, vol. 240, pp. 124860–124868, 2020.

[37] D. X. Liang, C. Y. Luo, X. Zhou, H. C. Chen, Y. W. Cheng, and S. H. Deng, "Adsorption of Cd^{2+} from aqueous solution by modified wheat chaff," *Journal of Agro-Environment Science*, vol. 34, no. 12, pp. 2364–2371, 2015.

[38] J. L. Gardea-Torresdey, J. H. Gonzalez, K. J. Tiemann, O. Rodriguez, and G. Gamez, "Phytofiltration of hazardous cadmium, chromium, lead and zinc ions by biomass of *Medicago sativa* (Alfalfa)," *Journal of Hazardous Materials*, vol. 57, no. 1–3, pp. 29–39, 1998.

[39] P. Gayatree, B. Raja, K. B. Sushanta, and B. C. Meikap, "Removal of dyes from aqueous solution by sorption with fly ash using a hydrocyclone," *Journal of Environmental Chemical Engineering*, vol. 6, no. 4, pp. 5204–5211, 2018.

[40] F.-C. Wu, R.-L. Tseng, and R.-S. Juang, "Kinetic modeling of liquid-phase adsorption of reactive dyes and metal ions on chitosan," *Water Research*, vol. 35, no. 3, pp. 613–618, 2001.

[41] I. Holford, "The comparative significance and utility of the Freundlich and Langmuir parameters of characterizing sorption and plant availability of phosphate in soils," *Soil Research*, vol. 20, no. 3, pp. 233–242, 1982.

[42] D. Mohan, C. U. Pittman, M. Bricka et al., "Adsorption of arsenic, cadmium, and lead by chars produced from fast pyrolysis of wood and bark during bio-oil production," *Journal of Colloid And Interface Science*, vol. 310, no. 1, pp. 57–73, 2007.

[43] S. Muthusamy, S. Venkatachalam, P. M. K. Jeevamani, and N. Rajarathinam, "Biosorption of Cr (VI) and Zn (II) ions from aqueous solution onto the solid biodiesel waste residue: mechanistic, kinetic and thermodynamic studies," *Environmental Science and Pollution Research International*, vol. 21, no. 1, pp. 593–608, 2014.

[44] F. Ma, S. P. Huang, and H. T. Du, "Preparation of a novel amphoteric bio-adsorbent using wheat straw and mechanism for removing Pb^{2+} and As^{5+} from aqueous solutions," *Transactions of the Chinese Society of Agricultural Engineering*, vol. 35, no. 20, pp. 210–219, 2019.

[45] C. Namasivayam and R. T. Yamuna, "Adsorption of direct red 12 B by biogas residual slurry: equilibrium and rate processes," *Environmental Pollution*, vol. 89, no. 1, pp. 1–7, 1995.

[46] H. Zhang, A. M. Omer, Z. H. Hu, L.-Y. Yang, C. Ji, and X.-K. Ouyang, "Fabrication of magnetic bentonite/carboxymethyl chitosan/sodium alginate hydrogel beads for Cu (II) adsorption," *International Journal of Biological Macromolecules*, vol. 135, pp. 490–500, 2019.

[47] P. Qu, Y. C. Li, H. Y. Huang et al., "Urea formaldehyde modified alginate beads with improved stability and enhanced removal of Pb^{2+}, Cd^{2+}, and Cu^{2+}," *Journal of Hazardous Materials*, vol. 396, pp. 122664–122693, 2020.

[48] Y. Y. Liu, L. Wang, X. Y. Wang, F. Q. Jing, R. H. Chang, and J. W. Chen, "Oxidative ageing of biochar and hydrochar alleviating competitive sorption of Cd (II) and Cu (II)," *Science of the Total Environment*, vol. 725, pp. 138419–138429, 2020.

[49] H. H. Du, W. L. Chen, P. Cai, X. M. Rong, X. H. Feng, and Q. Y. Huang, "Competitive adsorption of Pb and Cd on bacteria–montmorillonite composite," *Environmental Pollution*, vol. 218, pp. 168–175, 2016.

[50] Z. T. Li, L. Wang, J. Meng et al., "Zeolite-supported nanoscale zero-valent iron: new findings on simultaneous adsorption of Cd (II), Pb (II), and As (III) in aqueous solution and soil," *Journal of Hazardous Materials*, vol. 344, pp. 1–11, 2018.

[51] Z. L. Tian, L. P. Zhang, G. Shi, X. X. Sang, and C. H. Ni, "The synthesis of modified alginate flocculants and their properties for removing heavy metal ions of wastewater," *Journal of Applied Polymer Science*, vol. 135, no. 31, pp. 46577–46584, 2018.

[52] J. H. Chen, J. C. Ni, Q. L. Liu, and S. X. Li, "Adsorption behavior of Cd (II) ions on humic acid-immobilized sodium alginate and hydroxyl ethyl cellulose blending porous composite membrane adsorbent," *Desalination*, vol. 285, pp. 54–61, 2012.

[53] P. N. Fotsing, E. D. Woumfo, S. A. Măicăneanu et al., "Removal of Cu (II) from aqueous solution using a composite made from cocoa cortex and sodium alginate," *Environmental Science and Pollution Research*, vol. 27, no. 8, pp. 8451–8466, 2020.

[54] L. D. C. Alves, S. Yáñez-Vilar, Y. Piñeiro-Redondo, and J. Rivas, "Novel magnetic nanostructured beads for cadmium (II) removal," *Nanomaterials*, vol. 9, no. 3, p. 356, 2019.

[55] Y.-Y. Wang, W.-B. Yao, Q.-W. Wang, Z.-H. Yang, L.-F. Liang, and L.-Y. Chai, "Synthesis of phosphate-embedded calcium alginate beads for Pb (II) and Cd (II) sorption and immobilization in aqueous solutions," *Transactions of Nonferrous Metals Society of China*, vol. 26, no. 8, pp. 2230–2237, 2016.

[56] W. Zhang, H. Y. Wang, X. L. Hu et al., "Multicavity triethylenetetramine-chitosan/alginate composite beads for enhanced Cr (VI) removal," *Journal of Cleaner Production*, vol. 231, pp. 733–745, 2019.

[57] M. Y. Dai, Y. Liu, B. Z. Ju, and Y. Tian, "Preparation of thermoresponsive alginate/starch ether composite hydrogel and its application to the removal of Cu (II) from aqueous solution," *Bioresource Technology*, vol. 294, pp. 122192–122199, 2019.